Effect of Pretreatment of Nanocomposite PES-Fe$_3$o$_4$ Separator on Microbial Fuel Cells Performance

Irene Bavasso [ID],[1] Luca Di Palma,[1] Debora Puglia,[2] Francesca Luzi,[2] Franco Dominici [ID],[2] Jacopo Tirillò,[1] Fabrizio Sarasini [ID],[1] Luigi Torre[2]
[1]Department of Chemical Engineering Materials Environment & UdR INSTM, Sapienza-Università di Roma, Rome, Italy
[2]Department of Civil and Environmental Engineering & UdR INSTM, University of Perugia, Terni, Italy

Nanocomposite membranes based on polyethersulfone (PES) and nanomagnetite have been investigated with regards to the effect of pretreatments on the electrochemical performance of microbial fuel cells (MFCs). Nanocomposite membranes containing various amounts of Fe$_3$O$_4$ (5, 10, and 20 wt%) were characterized by Fourier transform infrared spectroscopy, scanning electron microscopy, thermogravimetric analysis, differential scanning calorimetry, and tensile tests. The application in MFC systems requires also chemical characterizations such as ion exchange capacity, water uptake, and oxygen permeability. The best formulation (PES10) showed electrochemical properties similar to the PES20. With the aim of obtaining a high-performance membrane with a low filler dosage, a pretreatment procedure (1 h of boiling step in deionized water and 1 h of immersion in 0.5 M of H$_2$SO$_4$) was adopted. The results of such pretreatment in terms of maximum power and current density were 10.59 ± 0.72 mW/m^2 and 52.07 ± 0.86 mA/m^2, respectively. The adoption of a pretreatment avoids the need of higher amount of nanofillers that can affect membrane surface roughness and its processing. Overall, the nanocomposite membranes represent a suitable technology in the MFC process. POLYM. ENG. SCI., 00:000–000, 2019. © 2019 Society of Plastics Engineers

INTRODUCTION

Microbial fuel cell (MFC) system is a well-known bioelectrochemical device where electrical energy is produced directly by electroactive bacteria from organic carbon rich wastewater [1], which still represents a potential renewable energy source alternative to fossil fuel based electricity. A typical dual chamber MFC consists in an anodic and cathodic chamber separated by a half-cell separator, which can be a proton exchange membrane (PEM) [2], salt bridge [3], or ceramic [4]. Cells based on PEMs are considered the optimal solutions in some applications, including backup power sources, power sources for portable electronics and distributed power generation [5]. In this regard, Nafion117 membrane is the most common commercial membrane due to the high ionic conductivity, which enhances the electrochemical properties of MFC, and mechanical/thermal stability [6]. On the other hand, the high cost of this material (~38% of the capital costs in MFC) [7] in addition to oxygen crossover and substrate loss [8, 9] has stimulated research toward alternative materials.

In an attempt to reduce the cost of MFC system, other polymer matrices have been proposed as alternatives to Nafion-based membranes (such as sulfonated polystyrene–ethylene–butylene–polystyrene, sulfonated PEEK, poly(vinylidene fluoride)–poly(styrene sulfonic acid)) [8, 10–12] and the addition of nanofillers proved to be an effective solution for the enhancement of the electrochemical properties of MFCs [13, 14]. In a previous work, polyethersulfone (PES)-Fe$_3$O$_4$ nanocomposites were tested in a dual-chamber MFC as an alternative separator and mechanical, thermal and electrochemical performances of neat PES, PES-Fe$_3$O$_4$ (5 and 20 wt%) were compared to those observed with commercial membranes (CMI 7000 and Nafion 117) [15]. Positive results in terms of mechanical and thermal stability were obtained, while maximum power and current density values for a PES with 20 wt% of Fe$_3$O$_4$ (PES20) were found to be slightly lower than those of commercial ones.

Proton conductivity in Nafion-related membranes is due to sulfonic acid groups that act as extremely effective proton donors, especially in the hydrolyzed form with water [16, 17]. This explains why Nafion membranes are usually pretreated before being used in MFCs. A common pretreatment reported in many experimental studies consists of three steps: (1) a first boiling in distilled water, (2) then in hydrogen peroxide, and (3) finally in a strong acid (HNO$_3$, H$_2$SO$_4$) [18–20]. The combination of these steps allows the removal of impurities and is required to provide a higher power density, columbic efficiency (CE) and chemical oxygen demand (COD) removal in a dual compartment MFC, as demonstrated by Ghasemi et al. [20]. The pretreated membrane was also able to reduce the biofouling tendency, which is another limiting factor in MFCs, leading to electrode surface blockage and ultimately a reduction in surface area [21]. Rough surfaces tend to foul easily due to increased surface area and when using polymer membranes doped with nanoparticles, the roughness increases with increasing amount of fillers [19]. This was confirmed also in our previous study [15], where for PES20 this aspect was likely suggested to limit the MFC performance by influencing the fouling tendency and the resulting internal resistance.

In the present study, it is speculated that an increase in membrane conductivity can counteract the increase in surface roughness due to nanoparticle amount, and for this reason a new content equal to 10 wt% of nano-Fe$_3$O$_4$ was used in PES matrix and all membranes were compared with and without pretreatments in terms of MFC electrochemical parameters during the treatment of sodium acetate as sole electron donor. To the best of authors' knowledge, the effects of pretreatment on this type of PEM in terms of mechanical, thermal, and morphological properties have not been addressed in literature. In addition, thermal and mechanical properties of pretreated membranes were compared with those of membranes after 360 h of MFC operation, thus paving the way for a more detailed understanding of the property–structure

relationships in nanocomposite membranes for their subsequent optimization as alternatives to Nafion membranes.

EXPERIMENTAL

Synthesis of Fe₃O₄ Nanoparticles and PES-Based Nanocomposite Membranes

Nanocomposite membranes with PES (Ultrason E3010 from BASF) as matrix and Fe_3O_4 nanoparticles as filler were prepared using the melt-blending technique. The chemical procedure adopted for the synthesis of magnetic nanoparticle was the coprecipitation of Fe^{2+} and Fe^{3+} with a molar ratio of 3:2 in ammonium hydroxide as precipitating agent, as fully described elsewhere [15, 22]. A new formulation with magnetite content of 10 wt% (PES10) in sheet form was prepared using a micro-extruder DSM Xplore 15 CC Micro Compounder coupled with a DSM Film Device as detailed in Ref. [15].

PEM Characterization

Differential scanning calorimetry (DSC; Mettler Toledo, 822e) measurements were performed in the temperature range from 25°C to 260°C at 10°C/min under nitrogen flow. PES and PES nanocomposite samples (6–8 mg) were heated from −25°C to 260°C at a rate of 10°C/min and held at 260°C for 2 min to erase the thermal history (first scan), then they were cooled to 25 at 10°C/min and reheated under the same conditions (second scan). Glass transition temperature was determined from the second heating scan. Fourier transform infrared (FTIR) measurements were performed at room temperature in reflection mode in attenuated total reflectance (ATR) using a JASCO FTIR 615 spectrometer. Spectra were acquired within 4,000–600 cm⁻¹ region, using 32 scans overlapped and 4 cm⁻¹ resolution.

PEM Morphological, Mechanical, and Thermal Characterization. Samples for the tensile characterization were cut from the films (thickness = 150–250 μm) in accordance with UNI EN ISO 527-2 (Type 1BA) with a gauge length of 30 mm. Tests were performed in displacement control on a universal testing machine Zwick/Roell Z010 with a crosshead speed of 10 mm/min. At least five tests were carried out at room temperature for each material formulation and pretreatment.

A SETSYS Evolution system by Setaram was used for the thermogravimetric analysis (TGA) of membranes in the temperature range from 25°C to 800°C with a heating rate of 10°C/min under nitrogen flow.

A contact profilometer Talyscan 150 by Taylor Hobson was used for measuring the surface roughness of the membranes and the corresponding R_a values were obtained by TalyMap software.

The morphology of membranes after MFC operation was investigated by scanning electron microscopy (Zeiss, Auriga). Specimens were sputter coated with chromium prior to observation.

Chemical and Electrochemical Characterization. Properties such as water uptake (W_{ut}), ion exchange capacity (IEC), and oxygen transfer coefficient (K_o) were determined. W_{ut} of the nanocomposite membranes was calculated as the difference between the wet weight (W_w), after immersion in deionized water at room temperature for 24 h, and dry weight (W_d), after vacuum drying at 100°C for 12 h, according to Eq. 1:

$$W_{ut}(\%) = \frac{W_w - W_d}{W_d} \cdot 100 \qquad (1)$$

IEC was determined by titration method [23] and calculated using Eq. 2:

$$IEC = \frac{V_{NaOH}(mL) \cdot \text{Normality of the titrant (NaOH)}}{\text{Weight of the dry membrane (g)}} \qquad (2)$$

K_o was determined directly in the H-type MFC. Each chamber was fed with distilled water and anodic chamber was supplied by the oxygen sensor (SEVENGO PRO-Mettler Toledo) while the cathodic chamber was continuously aerated. K_o (cm/s) was calculated using Eq. 3:

$$K_0 = -V/At \ln[(C_0 - C)/C_0] \qquad (3)$$

where V (mL) is the liquid volume in the anodic chamber, A (cm²) is the cross-sectional area of the membrane, t (s) is the time, and C_0 and C (mg/L) are the concentration of saturated oxygen in cathodic chamber and the dissolved oxygen concentration at time t, respectively.

The evaluation of the electrochemical performance of the membranes was conducted by placing the nanocomposites between the two cylindrical compartments (typical H-type MFC configuration) hermetically fixed by a clamp. The electrical resistance provided by the membrane was measured by a *test cell* where both chambers were equipped with a Pt electrode and filled with 0.05 mol/L sodium sulfate solution. Galvanostatic tests were conducted using current intensity (I) value in a range of 0–100 μA. Potential (E) values were recorded and the internal resistance (R) was obtained by using Ohm's law (Eq. 4):

$$R = \frac{E}{I} \qquad (4)$$

Open-circuit voltage (OCV) measurement and linear sweep voltammetry (LSV) technique (VSP Bio-Logic Potentiostat) were performed during the simulation of a synthetic wastewater treatment. The Pyrex glass anodic and cathodic compartments (each with a volume of 250 mL) were filled with the buffered [24] synthetic wastewater (pH = 7 measured by GLP21 Crison) using sodium acetate (2 g/L) and only buffer phosphate [25], respectively. Anaerobic digestion supernatant (2 mL) was used as microorganism source and inoculated in the anaerobic anode chamber. The aeration in the cathode chamber was maintained by an air diffusion system. Carbon paper electrodes were placed in both chambers and they were connected by a titanium wire closed by a resistor (180 Ω). A reference electrode (Ag/AgCl Crison 5240) was placed in the anodic compartment while an air diffuser was activated in cathodic chamber to enhance reduction reactions.

The sodium acetate removal was evaluated by total organic carbon measurement (TOC-L Analyzer, Shimadzu) and the corresponding CE was calculated using Eq. 5:

$$CE(\%) = \frac{M \int_0^t I \, dt}{F \, b \, V_{an} \, \Delta COD} \qquad (5)$$

where M is the molecular weight of the oxygen, I is the current over the time (t), F is the Faraday's constant, b is the number of

TABLE 1. Electrochemical performance of MFC using PES-based nanocomposite membranes.

Sample ID	P_{max} (mW m^{-2})	I_{max} (mA m^{-2})	OCV_{max} (mV)	Membrane resistance (kΩ)	Reference
PES5	1.66 ± 0.21	6.65 ± 0.86	485.00 ± 15.00	46.28 ± 2.91	[15]
PES5 pre	3.80 ± 0.54	15.23 ± 0.87	513.50 ± 9.75	32.86 ± 3.80	This study
PES10	5.72 ± 0.81	20.78 ± 0.30	550.50 ± 3.53	13.87 ± 1.79	This study
PES10 pre	10.59 ± 0.72	52.07 ± 0.86	555.00 ± 15.00	7.55 ± 2.19	This study
PES20	9.59 ± 1.18	38.38 ± 4.73	552.50 ± 29.50	8.88 ± 0.11	[15]

electrons exchanged per mole of oxygen ($b = 4$), COD identifies the chemical oxygen demand of the compounds present in the wastewater [26], and V_{an} is the anolyte volume. In case of sodium acetate, it was observed (data not reported) that the COD/TOC ratio is almost constant and equal to 2.8 ± 0.73. For this reason, Eq. 5 was adapted to use TOC values [27].

Membrane Pretreatments

According to the standard procedure adopted for Nafion 117 [20], the pretreatment was made by single steps or by the combination of different steps each of 1 h. Boiling water, H_2O_2 (3%) and H_2SO_4 (0.5 mol/L) are reagents commonly used for the pretreatment of Nafion-based or sulfonated polymers, as previously discussed. In our case, the effectiveness of these three chemicals at room and 100°C was investigated and the internal resistance through *test cell* was evaluated after each cycle.

RESULTS AND DISCUSSION

Characterization of PES10 Membrane

A preliminary characterization was performed on the new membrane formulation with a nanomagnetite content equal to 10 wt%. The water uptake is an important parameter for a membrane as it is directly linked to its proton conductivity [28]. PES10 exhibited a water uptake of $1.56\% \pm 0.24\%$, which is intermediate between the values of PES5 and PES20 membranes [15], thus confirming that this property is dependent on the addition of Fe_3O_4 nanoparticles, even if this value remained lower than the commercial membranes. The relatively hydrophobic character of PES [29] is likely its main disadvantage, as several studies have reported that membrane fouling is directly related to

hydrophobicity [30, 31]. IEC and K_0 values were calculated as 0.07 ± 0.02 meq/g and 1.26×10^{-3} cm/s, respectively. IEC value for PES10 membrane is lower than Nafion 117 but equal to another commercial membrane CMI-7000 and higher than PES5-PES20 membranes. The presence of sulfonic acid groups in magnetite nanoparticles could be beneficial to increase water uptake and IEC. Agglomeration of nanoparticles at a 20 wt% amount caused a decrease in IEC value [15], which is not observed in PES10, thus suggesting an homogeneous dispersion of Fe_3O_4 in the polymer matrix. This uniform dispersion resulted also in an increased oxygen transfer coefficient, even higher than that of PES20, due to enhanced void space in membranes caused by inorganic (magnetite) and organic (polymer) interspace [32]. These preliminary results suggest that only a further increase in filler content will not be able to lead to an increase in water uptake and a decrease in oxygen permeability coefficient, which is needed to reach anaerobic conditions in the anodic chamber [25].

In Table 1, the electrochemical parameters observed during the treatment of 2 g/L of sodium acetate and the results of LSV test are reported. The OCV trend (Fig. 1) exhibited by the MFC with PES10 as membrane was similar to that reported in our previous work [15]: after 360 h of MFC treatment, a TOC removal of 73.35% and a CE of 8.16% were calculated (Fig. 2). This result shows that PES20 can be still considered as the best performing nanocomposite membrane in our investigation.

Effect of Pretreatments on the Thermal, Mechanical, and Morphological Properties of Nanocomposite Membranes

In attempt to improve the electrochemical performance of the MFC based on nanocomposite membranes without increasing the content of nanoparticles due to enhanced agglomeration issues and costs, pretreatments were developed in this study and their effects investigated. As mentioned in our previous work [15], generally the pretreatment is not used for improving IEC [33], but can enhance the electrochemical properties during the MFC operation. Before addressing this issue, the effects of pretreatments on the thermomechanical properties of membranes were investigated. At first, the treatment with H_2O_2 was performed at 100°C (according to the procedure suggested for Nafion 117) and then also at room temperature. The use of H_2O_2 (3 wt%) at 100°C is not a viable pretreatment, as specimens underwent a significant embrittlement with occurrence of cracks (white arrow), as exemplified in Fig. 3 for a PES5 membrane. This treatment is usually recommended to remove the organic impurities from Nafion membranes and at the same time in order to gain more water molecules during the subsequent treatment steps. PES displays excellent mechanical properties and a good thermal stability [34], but its resistance to powerful oxidants, such as hydrogen peroxide,
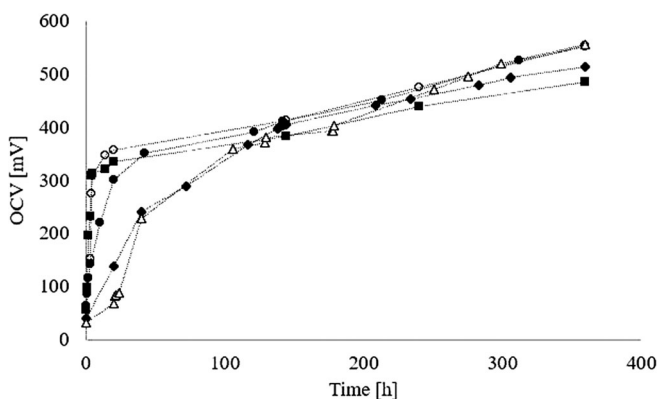

FIG. 1. OCV trends in PES10 without (●) and with pretreatment (△), PES 5 without (■) [15] and with pretreatment (◆), PES20 without pretreatment (○) [15].
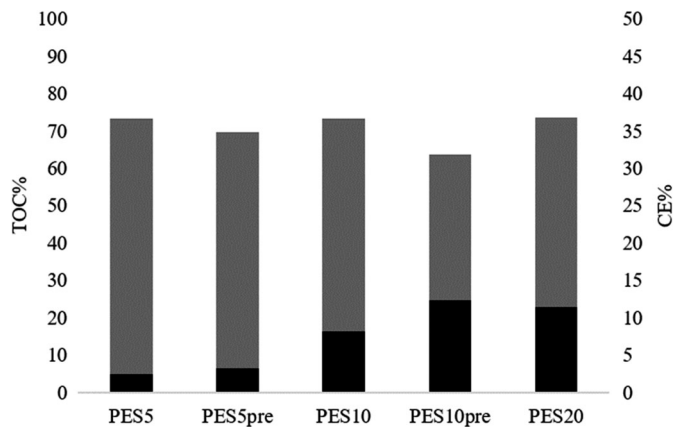
FIG. 2. Total organic carbon removal % (gray) and CE % (black) after 15 days of MFC operation.

FIG. 4. Weight loss as a function of temperature and nanoparticle amount for pretreated membranes. [Color figure can be viewed at wileyonlinelibrary.com]

can reduce the required membrane physicochemical properties due to a chemical degradation. The H_2O_2 attack is supposed to result in loss of the S═O bonds, with the conversion of the ─SO_2 group to charged ─SO_3 (sulfonate) groups [35], and related radicals attack on the PES [36]. Similar cracks on PES membranes were also reported after exposure to NaOCl [37, 38]. Reinforcing PES membranes with nanoparticles has been proposed as a strategy to minimize membrane degradation when exposed to strong oxidizing chemicals [35, 39]. The nanoparticles are supposed to act as decomposition catalysts, which minimize radical oxidative attack and degradation of membranes. In this study, Fe_3O_4 nanoparticles do not seem to be beneficial to resistance to chemical degradation induced by H_2O_2.

As already mentioned, conductivity in PEMs is related to the hydrophilic sulfonic groups that may be subjected to hydration, that is, water molecules may accumulate around these groups. In fact, water can hydrolyze the anhydrous form, SO_3H, to $SO_3^-H_3O^+$, allowing proton transport across the membrane [5]. A sulfonation process consists in the addition of sulfonic groups to the aromatic backbone of PES, through an electrophilic aromatic substitution reaction, even if PES is difficult to sulfonate because of the electron repulsing effect of the sulfonic group, which disables the aromatic rings for substitution [29]. Sulfuric acid is the
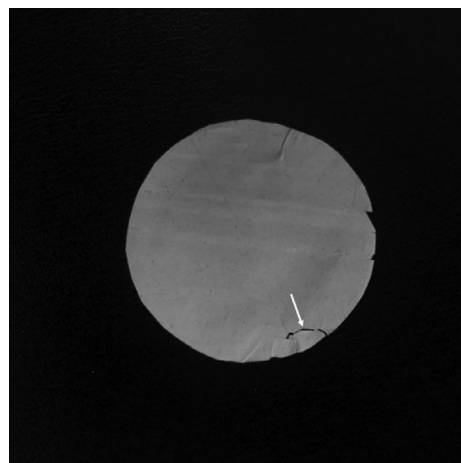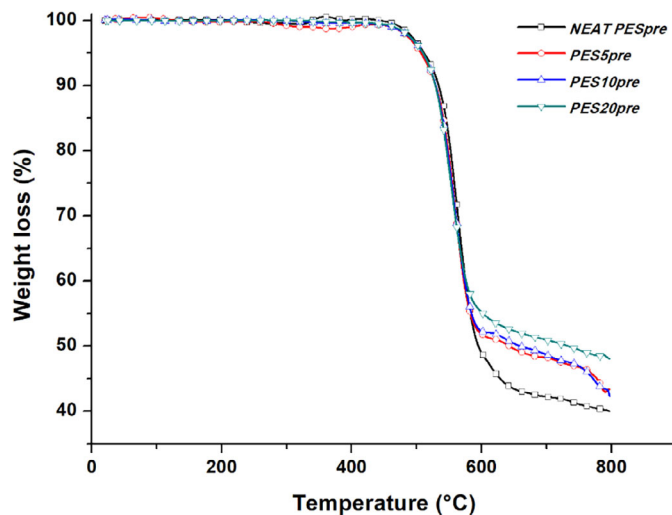
cheapest sulfonating agent but can lead to the degradation of the main polymer chain as a function of temperature (too high) and time (too long). This degradation can affect the mechanical resistance of the membrane, thus compromising its in-service properties. In this regard, sulfuric acid solution is commonly used for polymer sulfonation, but this step is generally preceded by a treatment at high temperature [33], which can act as a swelling step and can enhance the effectiveness of the subsequent H_2SO_4 step. In this study, a boiling step in deionized water for 1 h followed by 1 h immersion in the acid at room temperature was adopted.

TGA still showed a better thermal stability of pretreated nanocomposite membranes compared to commercial membranes [15] (Fig. 4). Pretreament did not alter the typical degradation pattern of PES, characterized by a single step related to chain random scission and carbonization to release SO_2 from the sulfone group and phenol from the ether group at the peak temperature [40]. When comparing the effect of the pretreatment for each formulation, the only significant difference was related to the final mass loss, which was found to decrease for pretreated samples, as shown in Fig. 5 for PES10 membranes. Results for other formulations showed the same response of PES10 membranes and the corresponding results were not included. The results suggest that the thermal stability was only marginally affected by the pretreatment steps that avoided the exposure to a strong oxidizing agent and the sulfonation at high temperature [29]. The degradation of the membrane after use and the presence of a biofilm are responsible for the slightly higher mass loss reported in Fig. 5.

In contrast, pretreatment markedly affected the tensile response of membranes, as can be inferred from the stress vs. strain curves and the relevant mechanical properties reported in Fig. 6. All pretreated membranes exhibited a higher ductility compared to untreated formulations, while strength and stiffness were reduced. The enhanced ductility can be related to a plasticizing effect due to the presence of increasing amount of water as a result of pretreatment. Generally, the glass transition can be considered as the range of temperatures at which segment motion of macromolecules becomes thermally activated and the shorter the segment length, the more flexible the macromolecular chains and the lower
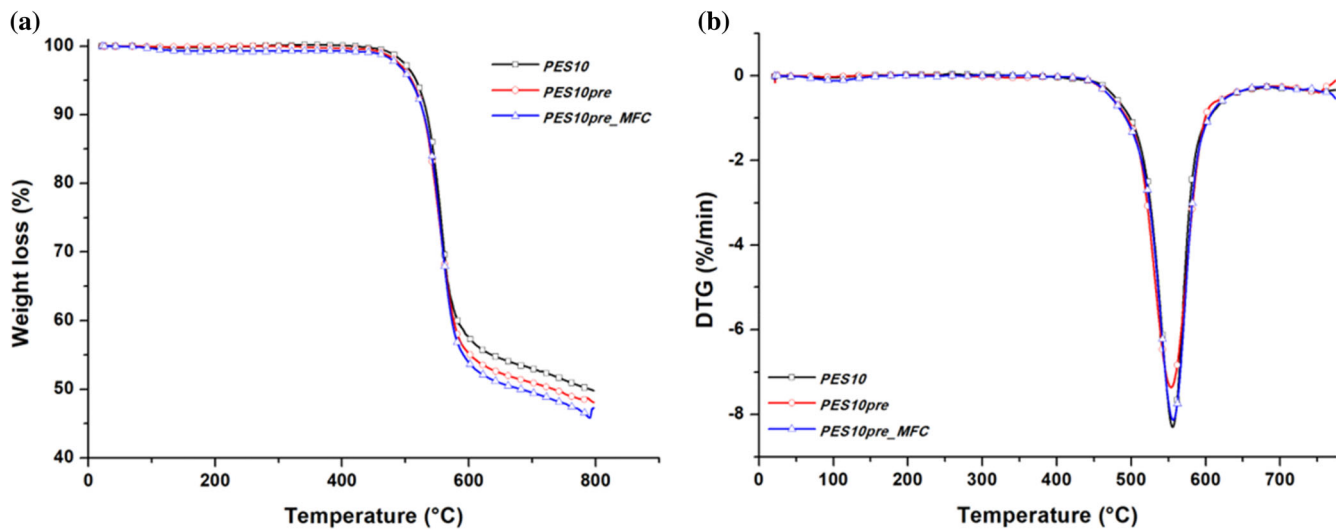

FIG. 3. Picture detailing the surface morphology of a PES5 membrane after H_2O_2 treatment.

FIG. 5.   (a) Weight loss and (b) DTG curves with temperature of virgin PES10, pretreated PES10 (PES10pre), and PES10 after MFC operation (PES10pre_MFC). [Color figure can be viewed at wileyonlinelibrary.com]
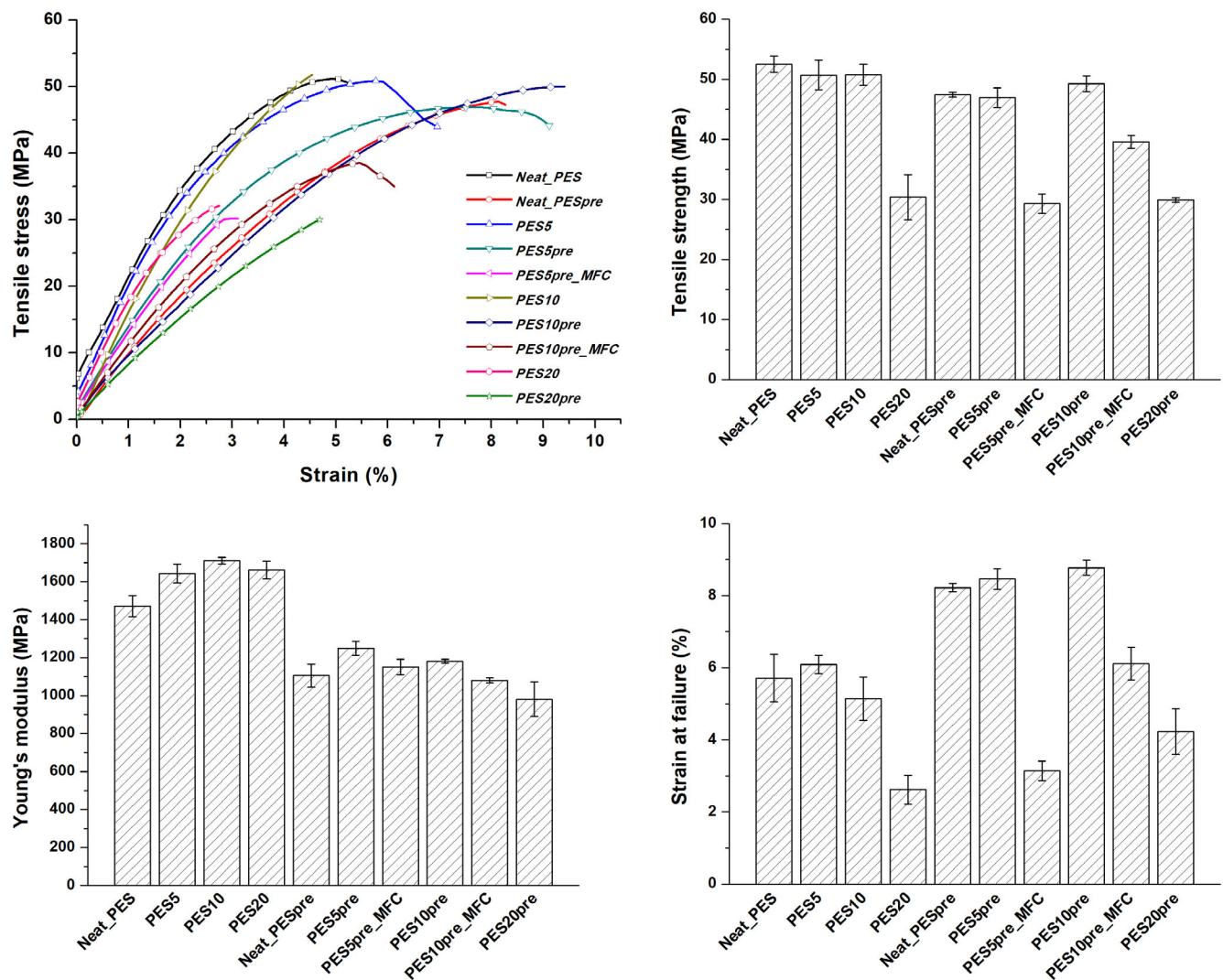

FIG. 6.   Typical stress versus strain curves from tensile tests for pretreated PES-based nanocomposites membranes and their tensile strength, Young's modulus, and strain at failure. [Color figure can be viewed at wileyonlinelibrary.com]

TABLE 2. Glass transition temperature of the different formulations.

Formulations	Second heating scan T_g (°C)
Neat PES	228[a]
Neat PESpre	224
PES5	230
PES5pre	226
PES5pre-MFC	226
PES10	234
PES10pre	227
PES10pre-MFC	229
PES20	234
PES20pre	231

[a]From TDS.

the T_g. Water can act as an effective plasticizer, shielding the intermacromolecular interactions and making easier the segmental molecular motion. This is usually described in terms of a reduced fracture strength and Young's modulus. DSC scans (Table 2) highlighted a decrease of glass transition temperature for all formulations, thus providing evidence of PES plasticization and, indirectly, of chemical functionalization of nanocomposite membranes, that is, the modification with sulfonic acid groups.

To this purpose, the surface chemistry and chemical composition of neat PES and PES/Fe$_3$O$_4$ systems after the treatment with H$_2$SO$_4$ were analyzed using ATR-FTIR in a wavenumber range of 400–4,000 cm^{-1}. For the sake of brevity, only spectra form PES10 membranes have been reported (Fig. 7). For all membranes, the absorption bands corresponding to the PES structure are observed at 1,580 cm^{-1} (benzene ring stretching), 1,488 cm^{-1} (C—C bond stretching), 1,244 cm^{-1} (aromatic ether stretching) and 1,106 cm^{-1} (C—O bond stretching), respectively [41]. A peak can be found at 574 cm^{-1} in the spectra of PES membranes with increasing content of Fe$_3$O$_4$ nanoparticles, that is associated with the stretching vibration mode of Fe—O. This band corresponds to intrinsic stretching vibrations of metal at the tetrahedral site [42, 43]. After surface treatment with sulfuric acid, ATR-FTIR spectra of PES-based membranes showed a more evident peak related to epoxy groups (C—O—C stretching at 1,200 cm^{-1}) and alkoxy groups (C—O stretching at 1,044 cm^{-1}) [44]. After the pretreatment, a weak shoulder at 1,019 cm^{-1} appeared, characteristic of the aromatic SO$_3$H
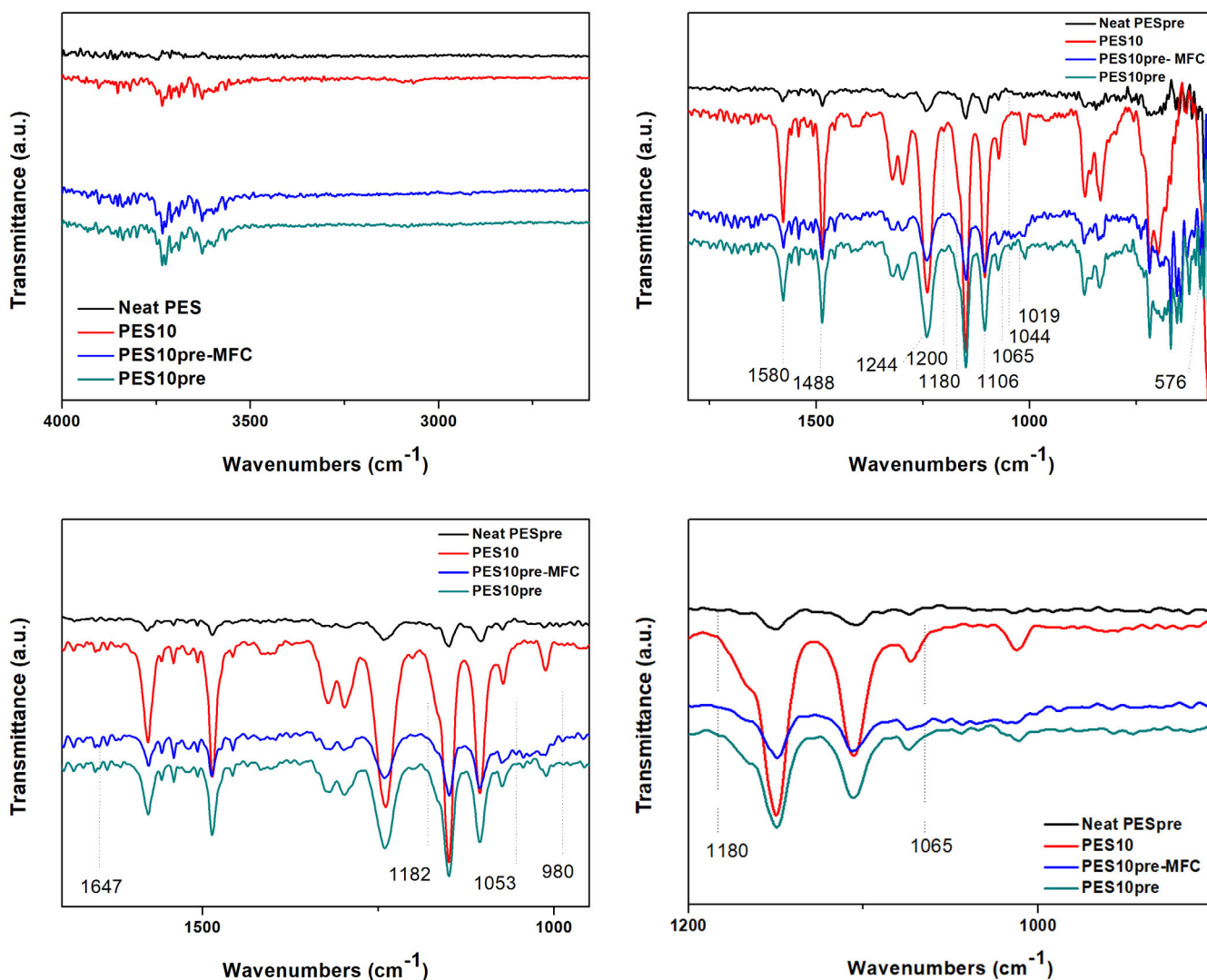

FIG. 7. FTIR spectra of PES10 membranes. [Color figure can be viewed at wileyonlinelibrary.com]
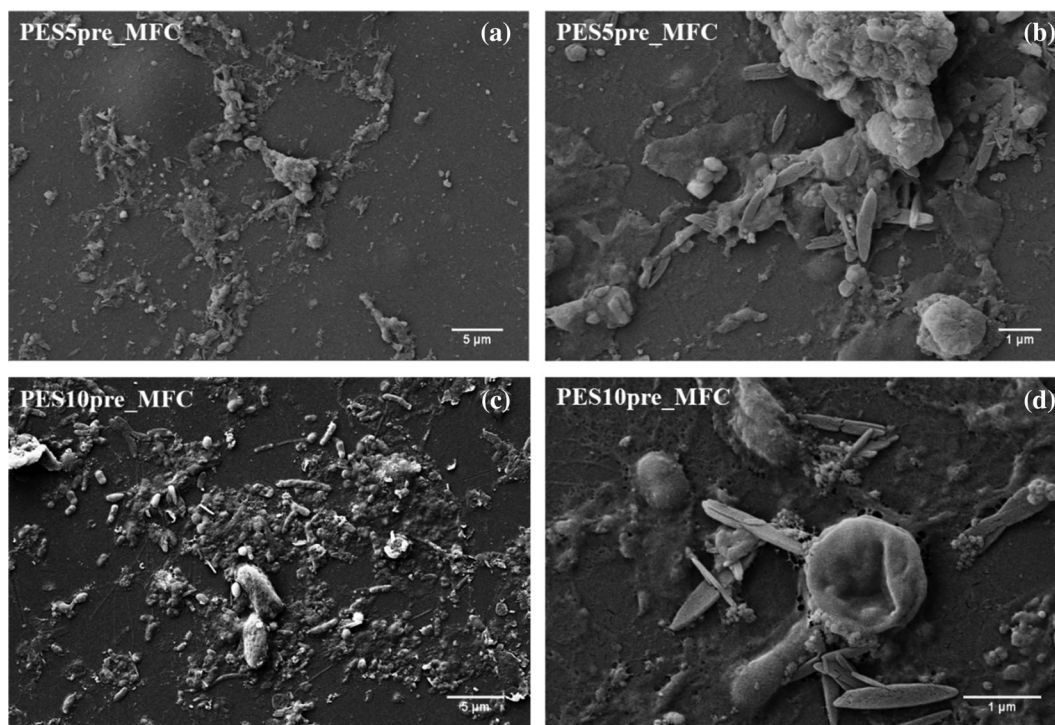
FIG. 8. SEM micrographs at two image magnifications of the fouling layer on PES5 (a,b) and PES10 (c,d) membranes after 15-day operation of MFC.

symmetric stretching vibrations. This absorption peak is absent in the PES spectrum and this confirms that the —SO_3H groups can be detected on PES membranes. Water molecules may easily accumulate around these groups. Absorption peak at 1,065 cm^{-1} can be also assigned to the C—O stretching band related to the C—O—SO_3 group [34].

MFC operation revealed the presence of several peaks on all the membrane spectra, indicating that the PES membranes were fouled by some contaminants (1,647 cm^{-1} due to stretching vibration of Amide I (C=O) and Amide II (—NH—) in proteins; 1,180 cm^{-1} as stretching vibration of C—N—C; 1,053 cm^{-1} due to the stretching vibration of S—O and 980 cm^{-1} as stretching vibration of C—O—C) [45]. This is also supported by SEM micrographs after MFC operation (Fig. 8), which displayed that the fouling layer consisted of microorganisms and some inorganic salt precipitations. With increasing nanofiller content from 5 wt% (Fig. 8a and b) to 10 wt% (Fig. 8c and d), the surface roughness was found to increase, and this resulted in a higher fouling tendency, as can be inferred from the presence of deposited material on the surface of the membrane exposed to the anodic compartment. This fouling connected to the roughness of the material is highlighted by comparing the figures at the same magnification (Fig. 8a–c) where is clearly evident a greater accumulation of deposit in PES10 (Fig. 8c) compared to PES5 (Fig. 8a) after the same operative time. The pretreatment roughened the membrane surface to a larger extent compared to untreated membranes, as clearly evident from the surface roughness images, and corresponding R_a values (Fig. 9). Surface roughness directly affects the fouling tendency and hinders the performance of the membrane, but at the same the formation of a thin biofilm on the surface can also have a beneficial effect on reducing the oxygen crossover from the cathodic chamber to the anodic one. This

enhances the anodic aerobic environment and better efficiency of the MFC as a whole can be expected [46]. In addition, the presence of an extended roughness can result in a higher nucleation of defects and stress concentration points on membranes, which can explain the further reduction in mechanical properties of membranes after MFC operation, especially in terms of strength, and the enhanced brittle character as extensive uniform elongations cannot be any longer sustained (Fig. 6).

MFC Performance

Pretreated PES5 and PES10 membranes were considered and compared with the optimal membrane obtained in a previous study (PES20) [15]. *Test cell* was considered as a measurement of the internal resistance in order to establish the best pretreatment before MFC application. As previously mentioned, the treatment involving hydrogen peroxide was discarded not only for its effects on the mechanical integrity of membranes, but also because an increase of 15% and 9% in internal resistance for PES5 and PES10 was observed, respectively. The same test performed at room temperature did not result in a decrease of the internal resistance (50.31 and 14.24 kΩ). Moreover, the treatments with H_2SO_4 0.5 mol/L at room temperature and at 100°C were not effective; on the contrary the boiling step with only deionized water resulted in a decrease of internal resistance of 14.13% and 24.36% for PES5 and PES10, respectively. After 1 h of boiling step in deionized water and 1 h of immersion in the acid at room temperature, a significant decrease of internal resistance was observed (Table 1), suggesting that 10 wt% as nanoparticle content can be considered as the optimal amount to be combined with a pretreatment. The same procedure was followed also for PES20, but no significant enhancements were
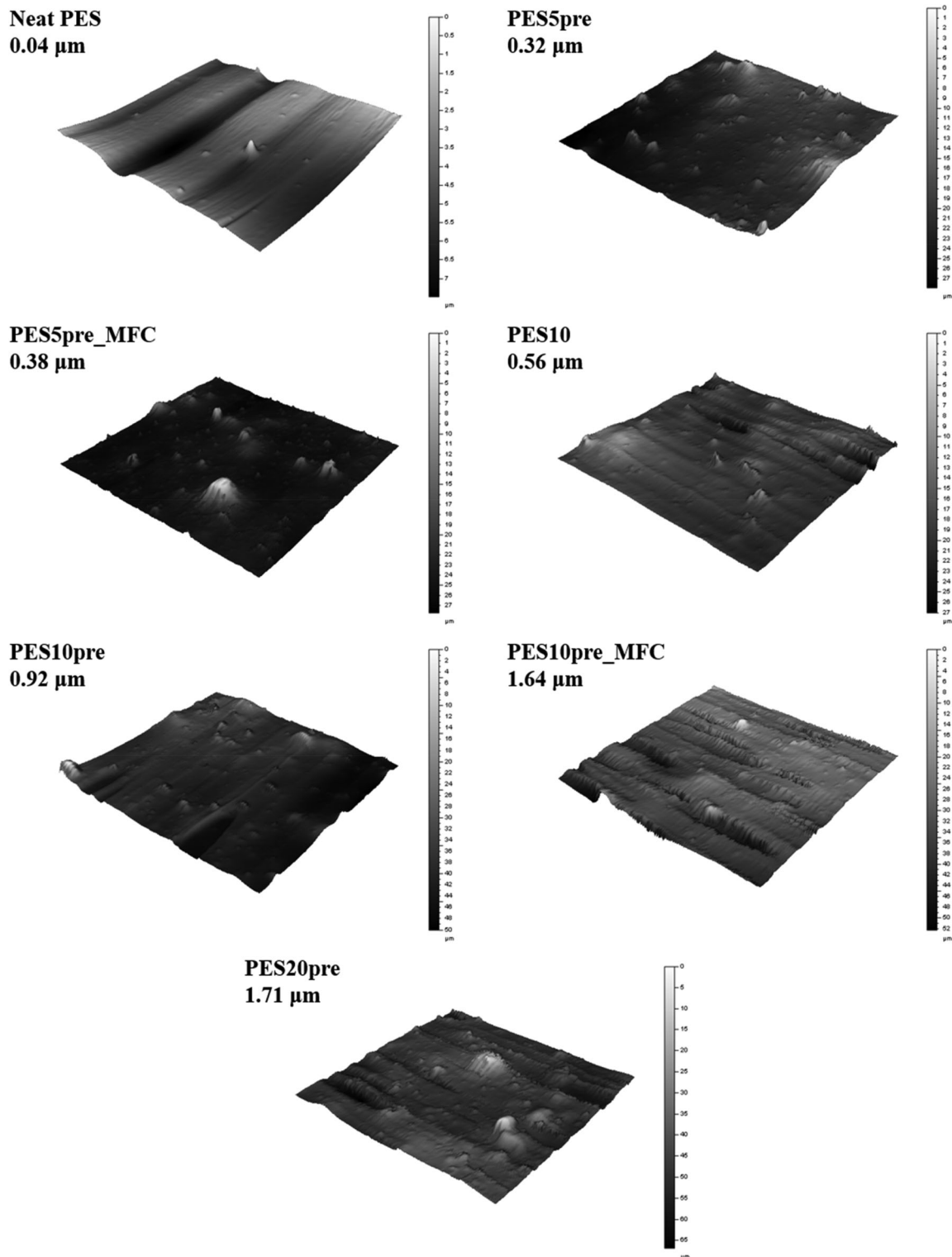
FIG. 9.   Surface roughness images of different nanocomposite membrane formulations and treatments.

observed, likely related to the lower IEC and agglomeration issues. The electrochemical properties of pretreated membranes were evaluated during the application of MFC system for wastewater remediation. After a treatment of 360 h of 2 g/L of sodium acetate, LSV measure was applied and the results are reported in Table 1. According to *test cell* also LSV results showed a positive enhancement of power and current density and in case of pretreated PES10 membranes, these values outperformed those exhibited by PES20. Similar organic carbon removal was observed with and without pretreatment but, although slightly, the CE observed with MFC coupled with pretreated PES10 was higher than PES20.

CONCLUSIONS

This study investigated a novel membrane based on PES and different amounts of nanomagnetite for MFCs. These membranes were manufactured by melt blending and extrusion and tested in an H-type MFC. In an attempt to improve the performance of MFC, different pretreatments were designed and tested, and their effects on mechanical, morphological, and thermal properties of membranes evaluated. A boiling step in deionized water for 1 h followed by 1 h immersion in H_2SO_4 (0.5 M) at room temperature did not compromise the thermal stability of the membranes but induced plasticization due to the increased water amount related to the sulfonation treatment, as confirmed by FTIR. This pretreatment was beneficial to the electrochemical performance of the MFC and an amount of 10 wt% of nanomagnetite showed the best compromise in terms of membrane resistance (7.55 kΩ), power density (10.59 mW/m) and mechanical properties. The pretreatment avoids the need of using higher amount of nanoparticles that degrade the mechanical properties of the membranes and significantly increase the surface roughness, potentially leading to higher biofouling tendency. Overall, the present investigation suggested that the incorporation of nanomagnetite fillers in pretreated nanocomposite membranes can be an effective tool to enhance the MFC performance. Future studies will be focused on tailoring the sulfonation of nanomagnetite to be used as effective proton conducting additives.

REFERENCES

1. D. Pant, G. Van Bogaert, L. Diels, and K. Vanbroekhoven, *Bioresour. Technol.*, **101**, 1533 (2010).

2. Z. Du, H. Li, and T. Gu, *Biotechnol. Adv.*, **25**, 464 (2007).

3. A. Pakash, S. Aziz, and S.A. Soomro, *J. Bioprocess. Biotechnol.*, **05**, 1 (2015).

4. V.M. Ortiz-Martínez, I. Gajda, M.J. Salar-García, J. Greenman, F.J. Hernández-Fernández, and I. Ieropoulos, *Chem. Eng. J.*, **291**, 317 (2016).

5. A. Kraytsberg and Y. Ein-Eli, *Energy Fuel*, **28**, 7303 (2014).

6. Q. Guo, P.N. Pintauro, H. Tang, and S. O'Connor, *J. Membr. Sci.*, **154**, 175 (1999).

7. X. Tang, K. Guo, H. Li, Z. Du, and J. Tian, *Biochem. Eng. J.*, **52**, 194 (2010).

8. S. Ayyaru, P. Letchoumanane, S. Dharmalingam, and A.R. Stanislaus, *J. Power Sources*, **217**, 204 (2012).

9. K.J. Chae, M. Choi, F.F. Ajayi, W. Park, I.S. Chang, and I.S. Kim, *Energy Fuel*, **22**, 169 (2008).

10. M. Rikukawa and K. Sanui, *Prog. Polym. Sci.*, **25**, 1463 (2000).

11. S. Ayyaru and S. Dharmalingam, *Bioresour. Technol.*, **102**, 11167 (2011).

12. S. Das, K. Dutta, and D. Rana, *Polym. Rev.*, **1**, 1 (2018).

13. A. Sivasankaran, D. Sangeetha, and Y.-H. Ahn, *Chem. Eng. J.*, **289**, 442 (2016).

14. M. Bazrgar and S.A. Mousavi, *Int. J. Hydrog. Energy*, **41**, 476 (2015).

15. L. Di Palma, I. Bavasso, F. Sarasini, J. Tirillò, D. Puglia, F. Dominici, and L. Torre, *Eur. Polym. J.*, **99** (2018).

16. S.C. DeCaluwe, A.M. Baker, P. Bhargava, J.E. Fischer, and J.A. Dura, *Nano Energy*, **46**, 91 (2018).

17. H.-G. Haubold, T. Vad, H. Jungbluth, and P. Hiller, *Electrochim. Acta*, **46**, 1559 (2001).

18. M. Cappadonia, J.W. Erning, S.M.S. Niaki, and U. Stimming, *Solid State Ion.*, **77**, 65 (1995).

19. M. Rahimnejad, M. Ghasemi, G.D. Najafpour, M. Ismail, A.W. Mohammad, A.A. Ghoreyshi, and S.H.A. Hassan, *Electrochim. Acta*, **85**, 700 (2012).

20. M. Ghasemi, W.R. Wan Daud, M. Ismail, M. Rahimnejad, A.F. Ismail, J.X. Leong, M. Miskan, and K. Ben Liew, *Int. J. Hydrog. Energy*, **38**, 5480 (2013).

21. A.J. Slate, K.A. Whitehead, D.A.C. Brownson, and C.E. Banks, *Renew. Sust. Energ. Rev.*, **101**, 60 (2019).

22. H. Shirinova, L. Di Palma, F. Sarasini, J. Tirillò, M.A. Ramazanov, F. Hajiyeva, D. Sannino, M. Polichetti, and A. Galluzzi, *Chem. Eng. Trans.*, **47**, 103 (2016).

23. C. Zhao, X. Li, H. Lin, K. Shao, and H. Na, *J. Appl. Polym. Sci.*, **108**, 671 (2008).

24. I. Bavasso, L. Di Palma, and E. Petrucci, *Chem. Eng. Trans.*, **47**, 223 (2016).

25. J.R. Kim, S. Cheng, S.-E. Oh, and B.E. Logan, *Environ. Sci. Technol.*, **41**, 1004 (2007).

26. M. Rahimnejad, A. Adhami, S. Darvari, A. Zirepour, and S.-E. Oh, *Alex. Eng. J.*, **54**, 745 (2015).

27. T. Kim, J. An, and J.K. Jang, *Bioresour. Technol.*, **195**, 217 (2015).

28. V. Barragán, C. Ruiz-Bauzá, J.P. Villaluenga, and B. Seoane, *J. Power Sources*, **130**, 22 (2004).

29. B. Van der Bruggen, *J. Appl. Polym. Sci.*, **114**, 630 (2009).

30. B. Van der Bruggen, L. Braeken, and C. Vandecasteele, *Sep. Purif. Technol.*, **29**, 23 (2002).

31. L. Braeken, K. Boussu, B. Van der Bruggen, and C. Vandecasteele, *ChemPhysChem*, **6**, 1606 (2005).

32. V. Kumar, P. Kumar, A. Nandy, and P.P. Kundu, *RSC Adv.*, **6**, 23571 (2016).

33. J.T.S. Allan, L.E. Prest, and E.B. Easton, *J. Membr. Sci.*, **489**, 175 (2015).

34. R. Guan, H. Zou, D. Lu, C. Gong, and Y. Liu, *Eur. Polym. J.*, **41**, 1554 (2005).

35. M.T. Tsehaye, J. Wang, J. Zhu, S. Velizarov, and B. Van der Bruggen, *J. Membr. Sci.*, **550**, 462 (2018).

36. R. Abejón, A. Garea, and A. Irabien, *Ind. Eng. Chem. Res.*, **52**, 17270 (2013).

37. K. Yadav, K. Morison, and M.P. Staiger, *Polym. Degrad. Stab.*, **94**, 1955 (2009).

38. M.T. Tsehaye, S. Velizarov, and B. Van der Bruggen, *Polym. Degrad. Stab.*, **157**, 15 (2018).

39. S. Xiao, H. Zhang, C. Bi, Y. Zhang, Y. Ma, X. Li, H. Zhong, and Y. Zhang, *J. Power Sources*, **195**, 8000 (2010).

40. P. Almén and I. Ericsson, *Polym. Degrad. Stab.*, **50**, 223 (1995).

41. S. Zhu, M. Shi, S. Zhao, Z. Wang, J. Wang, and S. Wang, *RSC Adv.*, **5**, 27211 (2015).

42. R. Yuvakkumar and S.I. Hong, *Adv. Mater. Res.*, **1051**, 39 (2014).

43. A. Demir, R. Topkaya, and A. Baykal, *Polyhedron*, **65**, 282 (2013).

44. T. Tomkovic, F. Radovanovic, B. Grgur, A. Nastasovic, D. Vasiljevic-Radovic, and A. Onjia, *J. Serb. Chem. Soc.*, **81**, 419 (2016).

45. S. Zhang, Y. Hui, and B. Han, in Proceedings of the 2015 International Conference on Mechatronics, Electronic, Industrial and Control Engineering, Atlantis Press, Paris, France (2015)

46. N.V. Prabhu and D. Sangeetha, *Chem. Eng. J.*, **243**, 564 (2014).